EFFECT OF SOLUTAL BUOYANCY FORCES ON THERMAL CONVECTION IN CONFINED NON-NEWTONIAN POWER-LAW FLUIDS

T. Makayssi*, M. Naïmi*[a], M. Lamsaadi*, M. Hasnaoui**, A. Raji*, A. Bahlaoui*

[*]Sultan Moulay Slimane university, Faculty of Sciences and Technologies, Physics Department, UFR of Sciences and Engineering of Materials, Team of Flows and Transfers Modelling (EMET), BP 523, Béni-Mellal, Morocco

[**]Cadi Ayyad University, Faculty of Sciences Semlalia, Physics Department, UFR TMF, Laboratory of Fluid Mechanics and Energetics (LMFE), BP 2390, Marrakech, Morocco

[a]Corresponding author. Tel.: (212) 23 48 51 12/22/82; Fax: (212) 23 48 52 01.
E-mail: naimi@fstbm.ac.ma, naimima@yahoo.fr

Received: 24 Sept 2007; accepted: 5 Nov 2007

This paper reports the results of an analytical and numerical study on natural convection heat transfer with and without solutal buoyancy forces in a non-Newtonian power-law fluid contained in a horizontal rectangular shallow enclosure submitted to uniform heat and mass fluxes along its short vertical sides, while the horizontal ones are insulated and impermeable. An approximate theoretical solution is developed, on the basis of the parallel flow assumption, and validated numerically by solving the full governing equations. A comparison between results obtained in presence and in absence of solutal buoyancy forces is done. The effect of the non-Newtonian behavior on fluid flow and heat transfer characteristics is examined.

Keywords: thermodynamic analysis in renewable energy, thermal natural convection, double diffusive convection, rectangular enclosures, non-Newtonian fluids

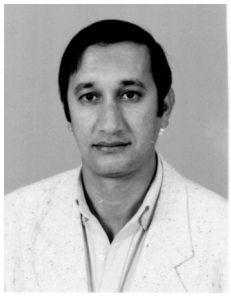

Mohamed Naïmi

Education: A national doctorate (INPL, Nancy, France, 1989) and a doctorate of state (University Cadi Ayyad, Marrakech, Morocco, 2001). The title of the former is: "Etudes des lois d'écoulement et de transfert de chaleur pour des fluides non-Newtoniens en espace annulaire tournant: approche réaliste de l'échangeur de chaleur à surface raclée" while the latter entitled: "Contribution à l'étude de l'effet Marangoni thermique dans les fluides non-Newtoniens en conditions de gravité et de microgravité".
Experience: A teacher researcher, with the degree of higher teaching Professor, at the Faculty of Sciences and Technologies of Sultan Moulay Slimane University (Béni-Mellal, Morocco).
Main range of scientific interests: natural, double diffusive and capillary convections in non-Newtonian fluids.
Publications: 8 main papers since 2005.

Nomenclature

A – aspect ratio of the cavity, Eq. (11)
C_T – dimensionless temperature gradient in the x-direction
C_S – dimensionless concentration gradient in the x-direction
D – mass diffusivity (m^2/s)
g – gravitational acceleration (m/s^2)
H' – height of the enclosure (m)
j' – constant mass flux per unit area ($kg/m^2 \cdot s$)
K – consistency index for a power-law fluid at the reference temperature ($Pa \cdot s^n$)
Le – Lewis number, Eq. (11)
L' – length of the rectangular enclosure (m)
N – buoyancy ratio, Eq. (11)
n – flow behavior index for a power-law fluid at the reference temperature
Nu – local Nusselt number, Eqs. (12), (13) and (33)
$\overline{Nu}$ – average Nusselt number, Eqs. (14) and (33)
Pr – generalised Prandtl number, Eq. (11)
q' – constant heat flux per unit area (W/m^2)
Ra_T – generalized thermal Rayleigh number, Eq. (11)
S – dimensionless concentration $\left[= \left(S' - S'_c\right) / \Delta S^*\right]$
S'_c – reference concentration at the geometric center of the enclosure (kg/m^3)
Sh – local Sherwood number, Eqs. (12), (13) and (33)
$\overline{Sh}$ – mean Sherwood number, Eqs. (14) and (33)
T – dimensionless temperature $\left[= \left(T' - T'_c\right) / \Delta T^*\right]$
T'_c – reference temperature at the geometric center of the enclosure (K)
ΔT^* – characteristic temperature $\left[= q'H'/\lambda\right]$ (K)
ΔS^* – characteristic concentration $\left[= j'H'/D\right]$ (kg/m^3)
(u, v) – dimensionless axial and transverse velocities $\left[= (u', v') / (\alpha / H')\right]$
(x, y) – dimensionless axial and transverse co-ordinates $\left[= (x', y') / H'\right]$

Greek symbols

α – thermal diffusivity of fluid at the reference temperature (m^2/s)

β_T – thermal expansion coefficient of fluid at the reference temperature (1/K)

β_S – solutal expansion coefficient of fluid at the reference concentration (m^3/kg)

λ – thermal conductivity of fluid at the reference temperature (W/m·C)

μ – dynamic viscosity for a Newtonian fluid at the reference temperature (Pa·s)

μ_a – dimensionless apparent viscosity of fluid, Eq. (7)

ρ – density of fluid at the reference temperature (kg/m^3)

Ω – dimensionless vorticity $\left[=\Omega/\left(\alpha/H'^2\right)\right]$

ψ – dimensionless stream function $\left[=\psi/\alpha\right]$

Superscript

′ – dimensional variable

Subscripts

c – value relative to the centre of the enclosure $(x, y) = (A/2, 1/2)$

* – characteristic variable

Introduction

Thermal or simple natural convection is a flow due to density variations with temperature in gravitational field. Double-diffusive natural convection, i.e. flows generated by buoyancy due to simultaneous temperature and concentration gradients, can be found in wide range of situations. In nature, such flows are encountered in the oceans, lakes, solar ponds, shallow coastal waters and the atmosphere. In industry, examples include chemical processes, crystal growth, energy storage, material and food processing, etc... For a review of the fundamental works in this area see, for instance, [1].

The literature on double-diffusive natural convection shows that the majority of investigations were focused on the enclosures of rectangular form [2].

In the past, many studies concerning Newtonian fluid flows in enclosures, driven simultaneously by thermal and solutal buoyancy effects, were carried out. These can be classified under three types, according to the thermal and solutal boundary conditions adopted. In the first type, the cavity is subjected to a vertical solutal gradient and a horizontal thermal one [3]. In the second type, both the temperature and concentration gradients are imposed transversally [4]. In the third type, which is the present case, both the thermal and solutal gradients are imposed laterally [5].

To our knowledge, for non-Newtonian fluids, except the work performed by Benhadji et al. [6] in the case of a porous horizontal rectangular layer, where double-diffusive convection is generated inside a power-law fluid by application of horizontal or vertical uniform heat and mass fluxes, there is no investigations dealing with fluid-filled enclosures.Otherwise, the majority of investigations concerning non-Newtonian fluids dealt with thermal driven buoyancy convection [7, 8].

Non-Newtonian flows are of importance and very present in many industrial applications such as paper making, oil drilling, slurry transporting, food processing, polymer engineering and many others. Some of these applications are discussed in Jaluria [9].

In order to contribute to fill the gap left by the lack of studies on the field, at least partly, the present investigation focuses on the effect of solutal buoyancy forces on natural convection heat transfer inside a two-dimensional horizontal rectangular enclosure, filled with a non-Newtonian fluid. The cavity is submitted to uniform heat and mass fluxes from its short vertical sides, while its long horizontal boundaries are insulated and impermeable.

Mathematical formulation

The studied configuration, sketched in Fig. 1, is a rectangular enclosure of height H' and length L' with the long horizontal rigid walls insulated and impermeable and the short vertical ones submitted to constant heat and mass densities of fluxes, q' and j', respectively.

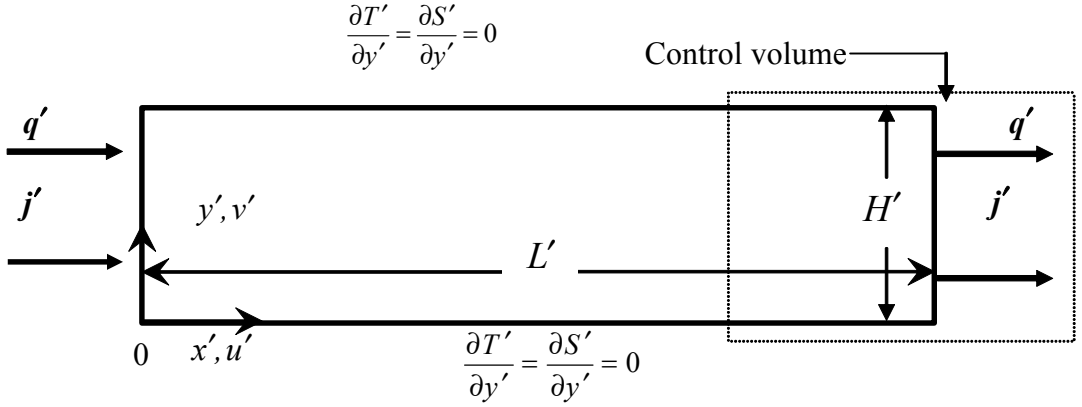

Fig. 1. *Sketch of the cavity and co-ordinates system*

The non-Newtonian fluids considered here are those for which the rheological behavior can be described by the power-law model, proposed by Ostwald-De Waele [10], whose expression, in term of laminar apparent viscosity, is

$$\mu'_a = k\left(2\left(\left(\frac{\partial u'}{\partial x'}\right)^2+\left(\frac{\partial v'}{\partial y'}\right)^2\right)+\left(\frac{\partial u'}{\partial y'}+\frac{\partial v'}{\partial x'}\right)^2\right)^{\frac{n-1}{2}}, \quad (1)$$

where n is the power-law index and k is an empirical coefficient known as the consistency factor, which is an indicator of the degree of fluids viscosity. Note that for $n = 1$ the power-law model reduces to the Newton's law by setting $k = \mu$. Thus, the deviation of n from unity characterizes the degree of non-Newtonian behavior of the fluid. Specifically, when n is in the range $0 < n < 1$ the fluid is said to be pseudo-plastic (or shear-thinning) and the viscosity is found to decrease by increasing the shear rate. On the other hand when $n > 1$ the fluid is said to be dilatant (or shear-thickening) and the viscosity increases by increasing the shear rate. Dilatant fluids are generally much less frequent than pseudo-plastic ones. Though the Ostwald-de Wale model does not converge to a Newtonian behavior in the limit of zero and maximum shear rates, it presents however the advantage to be simple and mathematically tractable. In addition, the rheological behavior of many substances can be adequately represented by this model for relatively large range of shear rates (or shear stresses) making it useful, at least for engineering purpose, and justifying its use in most theoretical investigations of fluids having pseudo-plastic or dilatant behaviors. On the other hand, the main assumptions made here are those commonly used, i.e., the flow is laminar and two-dimensional, the viscous dissipation is negligible, the interactions between heat and mass exchanges, known under the name of Soret and Duffour effects, are negligible, the fluid is incompressible and its physical properties are considered temperature independent except the density in the buoyancy term which obeys the Boussinesq approximation. Then, the dimensionless governing equations, written in terms of vorticity, Ω, temperature, T, concentration, S, and stream function, ψ, are:

$$\frac{\partial \Omega}{\partial t}+\frac{\partial(u\Omega)}{\partial x}+\frac{\partial(v\Omega)}{\partial y}=$$

$$=Pr\left[\mu_a\nabla^2\Omega+2\left[\frac{\partial\mu_a}{\partial x}\frac{\partial\Omega}{\partial x}+\frac{\partial\mu_a}{\partial y}\frac{\partial\Omega}{\partial y}\right]\right]+S_\Omega \quad (2)$$

$$\frac{\partial T}{\partial t}+\frac{\partial(uT)}{\partial x}+\frac{\partial(vT)}{\partial y}=\nabla^2 T \quad (3)$$

$$\frac{\partial S}{\partial t}+\frac{\partial(uS)}{\partial x}+\frac{\partial(vS)}{\partial y}=\frac{1}{Le}\nabla^2 S \quad (4)$$

and

$$\nabla^2\psi=-\Omega, \quad (5)$$

where

$$u=\frac{\partial\psi}{\partial y};\ v=-\frac{\partial\psi}{\partial x} \quad (6)$$

$$\mu_a=\left[2\left[\left(\frac{\partial u}{\partial x}\right)^2+\left(\frac{\partial v}{\partial y}\right)^2\right]+\left[\frac{\partial u}{\partial y}+\frac{\partial v}{\partial x}\right]^2\right]^{\frac{n-1}{2}} \quad (7)$$

and

$$S_\Omega=Pr\left[\left[\frac{\partial^2\mu_a}{\partial x^2}-\frac{\partial^2\mu_a}{\partial y^2}\right]\left[\frac{\partial u}{\partial y}+\frac{\partial v}{\partial x}\right]-2\frac{\partial^2\mu_a}{\partial x\partial y}\left[\frac{\partial u}{\partial x}-\frac{\partial v}{\partial y}\right]\right]+$$

$$+PrRa_T\left(\frac{\partial T}{\partial x}+N\frac{\partial S}{\partial x}\right). \quad (8)$$

Such a formulation presents the advantage to reduce the number of equations, by eliminating the pressure, which is without interest in this study, and to be more appropriate for two-dimensional flows.

The dimensionless boundary conditions, for the physical system considered here, are

$$u=v=\psi=0,\ \ \frac{\partial T}{\partial x}=\frac{\partial S}{\partial x}=1 \ \text{ for } x=0 \text{ and } A \quad (9)$$

$$u=v=\psi=0,\ \ \frac{\partial T}{\partial y}=\frac{\partial S}{\partial y}=0 \ \text{ for } y=0 \text{ and } 1 \quad (10)$$

On the other hand, for the vorticity, which is unknown at the boundaries, the relation of woods [11] is used, for its accuracy and stability.

The dimensionless variables are obtained by using the characteristic scales H', H'^2/α, α/H', α/H'^2, $q'H'/\lambda$, $j'H'/D$ and α corresponding to length, time, velocity, vorticity, characteristic temperature, characteristic concentration, and stream function, respectively.

In addition to the power-law index, n, the present problem is governed by five other dimensionless parameters, namely, the aspect ratio of the enclosure, A, the Lewis number, Le, the buoyancy ratio, N, the generalized Prandtl, Pr, and thermal Rayleigh, Ra_T, numbers, whose expressions are

$$A=\frac{L'}{H'},$$

$$Le=\frac{\alpha}{D},$$

$$N=\frac{\beta_S\Delta S^*}{\beta_T\Delta T^*},$$

$$Pr = \frac{(k/\rho)\,H'^{2-2n}}{\alpha^{2-n}}$$

and

$$Ra_T = \frac{g\beta H'^{2n+2} q'}{(k/\rho)\alpha^n \lambda}. \qquad (11)$$

Notice that it is possible to recover the Newtonian expressions of Pr and Ra_T by setting n = 1 and replacing k by the Newtonian viscosity μ.

Numerics

The two-dimensional governing equations are solved by using the well known second order central finite difference method with a regular mesh size. The integration of Eq. (2), (3) and (4), is performed with the alternating-direction implicit method (ADI). This method, frequently used for Newtonian fluids, was successfully extended to non-Newtonian power-law fluids in the past by Ozoe and Churchill [7] and recently by Lamsaadi et al. [8]. To satisfy the mass conservation, Eq. (5) is solved by a point successive over-relaxation method (PSOR) with an optimum relaxation factor calculated by the Franckel formula [11]. The mesh size is chosen on the basis of a compromise between running time and accuracy of the results. The procedure is based on grid refinement until the numerical results agree with the parallel flow ones, presented below, within reasonable accuracy. Hence, a uniform grid of 321×81 is found sufficient to model accurately the flow, temperature and concentration fields within a cavity of A = 24 (value used for the numerical computations). To satisfy the continuity equation, the convergence criterion $\sum_{i,j} \left|\psi_{i,j}^{k+1} - \psi_{i,j}^{k}\right| < 10^{-4} \sum_{i,j} \left|\psi_{i,j}^{k+1}\right|$ is adopted, where $\psi_{i,j}^{k}$ is the value of the stream function at the kth iteration level. The time step size, δt, is varied in the range $10^{-7} \le \delta t \le 10^{-4}$, depending on the values of the governing parameters. More precisely, the small values of δt are used for high values of n and Ra_T.

With the Ostwald power-law model, the dimensionless viscosity, given by Eq. (7), tends towards infinity, for, $0 < n < 1$ at the level of the cavity corners, where the velocity gradients tend towards zero, which renders impossible direct numerical computations. This difficulty is, however, overcome by using average values for the corner viscosity making, thus, the computations possible and stable.

The local heat and mass transfers through the fluid layer filling the cavity can be expressed in terms of the local Nusselt and Sherwood numbers, respectively, defined as

$$Nu(y) = \frac{q'}{(\lambda \Delta T'/L')} = \frac{A}{\Delta T} = \frac{1}{(\Delta T/A)}$$

and

$$Sh(y) = \frac{j'}{(D\,\Delta S'/L')} = \frac{A}{\Delta S} = \frac{1}{(\Delta S/A)}, \qquad (12)$$

where $\Delta T = T(0,y) - T(A,y)$ and $\Delta S = S(0,y) - S(A,y)$ are the side to side dimensionless local temperature and concentration differences, respectively. This definition is, however, notoriously inaccurate owing to the uncertainty of the temperature and concentration values evaluated at the two vertical walls (edge effects). Instead, the Nusselt and Sherwood numbers are calculated on the basis of a temperature and concentration differences between two vertical sections, far from the end sides. Thus, by analogy with Eq. (12), and considering two infinitesimally close sections, the local Nusselt and Sherwood numbers can be defined by

$$Nu(y) = \lim_{\delta x \to 0} \delta x/\delta T = \lim_{\delta x \to 0} \frac{1}{\delta T/\delta x} = -\frac{1}{(\partial x/\partial T)_{x=A/2}}$$

and

$$Sh(y) = \lim_{\delta x \to 0} \delta x/\delta S = \lim_{\delta x \to 0} \frac{1}{\delta S/\delta x} = -\frac{1}{(\partial x/\partial S)_{x=A/2}}, \qquad (13)$$

where δx is the distance between two symmetrical sections with respect to the central one. The corresponding average Nusselt and Sherwood numbers are, respectively, calculated at different locations, as follows

$$\overline{Nu} = \int_0^1 Nu(y)\,dy$$

and

$$\overline{Sh} = \int_0^1 Sh(y)\,dy. \qquad (14)$$

As an additional check of the results accuracy, energy and matter balances are systematically verified for the system at each numerical code running. Thus, the overall heat and mass transfers, through each vertical plane, are evaluated and compared with the quantities of heat and mass furnished to the system at x = 0. For the results reported here, the energy and matter balances are satisfied within 2 % as a maximum difference.

Typical numerical results, in terms of streamlines (a), isotherms (b) and isoconcentrations, are presented in Fig. 2, obtained, for A = 24, Le = 10, $Ra_T = 10^5$ and various values of n and N. As appears, from these figures, the flow is parallel to the horizontal boundaries of the enclosure and the temperature and the concentration are linearly stratified in the x-direction of the core region. The approximate analytical solution, developed in the next section, relies on these observations.

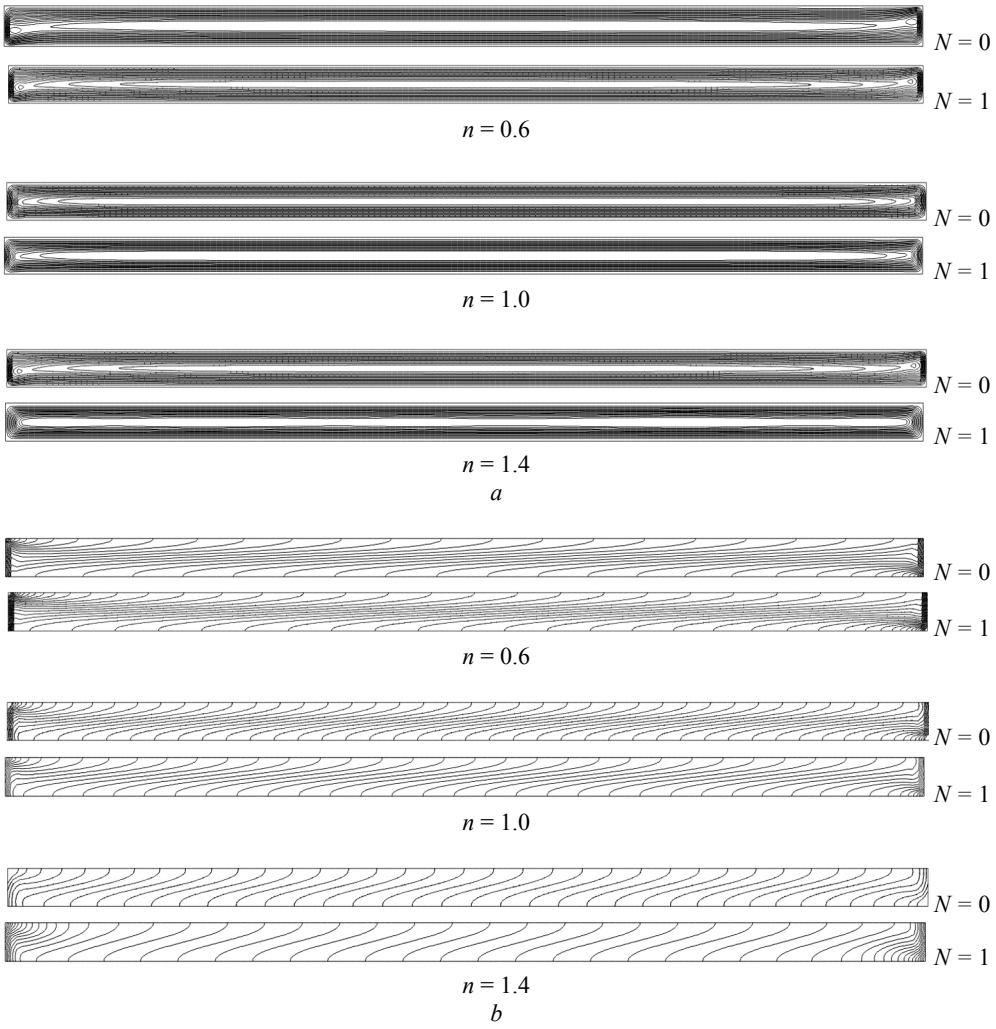

Fig. 2. *Combined effect of N and n on: a) – streamlines; b) – isotherms*

Approximate parallel flow analytical solution

The results presented in Fig. 2, allow the following appropriate simplifications:

$$\psi(x,y)=\psi(y),\ T(x,y)=C_T(x-A/2)+\theta_T(y)$$

and

$$S(x,y)=C_S(x-A/2)+\theta_S(y), \qquad (15)$$

where C_T and C_S are unknown constant temperature and concentration gradients in the x-direction. On the basis of this, the non-dimensional governing equations become

$$\frac{d^2}{dy^2}\left[\left|\frac{du}{dy}\right|^{n-1}\frac{du}{dy}\right]=(C_T+NC_S)Ra_T=ERa_T, \qquad (16)$$

$$C_T u=\frac{d^2\theta_T}{dy^2} \text{ and } LeC_S u=\frac{d^2\theta_S}{dy^2} \qquad (17)$$

with

$$u=\frac{d\theta_T}{dy}=\frac{d\theta_S}{dy}=0 \text{ for } y=0 \text{ and } 1, \qquad (18)$$

$$\int_0^1 u(y)\,dy=0 \qquad (19)$$

as boundary and return flow conditions, respectively.

Recently, the above concept has been successfully used by Lamsaadi et al. [8] to predict the thermal convection flow behavior in the case of a non-Newtonian power-law fluid.

The integration of Eq. (16) and (17), coupled with the conditions (18) and (19), leads to analytical expressions of velocity, temperature and concentration. However, such an operation is difficult to carry out owing to the particular nature of the governing equations and requires, therefore, a special numerical treatment. In fact, the non-linearity of the fluid behavior and the change of du/dy sign, due to the return flow, impose that the velocity

expressions are different depending on whether $0 \le y \le y_0$, $y_0 \le y \le y_1$ or $y_1 \le y \le 1$, where y_0 and $y_1 = 1 - y_0$ (because of the centro-symmetry of the core flow) are the vertical coordinate values for which $du/dy = 0$. They are derived from Eq. (19), which is numerically solved by using a combination of the Regula-Falsi iteration method [12] and the Gauss-Legendre integration method [13]. To reduce the velocity, temperature and concentration expressions, the function $f(y) = \left(y^2 - y + y_0 y_1\right)/2$ is introduced. Thus, for

$0 \le y \le y_0$

$$u(y) = E^{1/n}\ Ra_T^{1/n}\left[\int_0^y [f(y)]^{1/n}\,dy\right], \tag{20}$$

$$\theta_T(y) = C_T E^{1/n} Ra_T^{1/n}\left[\int_0^y\left[\int_0^y\left[\int_0^y [f(y)]^{1/n}\,dy\right]dy\right]dy\right] + \theta_T(0)\,. \tag{21}$$

$y_0 \le y \le y_1$

$$u(y) = E^{1/n}\ Ra_T^{1/n}\left[\int_0^y [f(y)]^{1/n}\,dy + \int_y^y [-f(y)]^{1/n}\,dy\right], \tag{22}$$

$$\theta_T(y) = C_T E^{1/n}\ Ra_T^{1/n}\left[\frac{(y-y_0)^2}{2}\int_0^{y_0}[f(y)]^{1/n}\,dy + \int_{y_0}^y\left[\int_{y_0}^y\left[\int_y^{y_0}[-f(y)]^{1/n}\,dy\right]dy\right]dy\right] +$$
$$+ (y-y_0)\int_0^{y_0}\left[\int_0^y [f(y)]^{1/n}\,dy\right]dy + \int_0^y\left[\int_0^y\left[\int_0^y [f(y)]^{1/n}\,dy\right]dy\right]dy\right] + \theta_T(0)\,. \tag{23}$$

$y_1 \le y \le 1$

$$u(y) = E^{1/n}\ Ra_T^{1/n}\left[\int_0^{y_0} [f(y)]^{1/n}\,dy + \int_{y_1}^{y_0} [-f(y)]^{1/n}\,dy + \int_{y_1}^y [f(y)]^{1/n}\,dy\right], \tag{24}$$

$$\theta_T(y) = C_T E^{1/n}\ Ra_T^{1/n}\left[\frac{1}{2}(y-y_1)(y+y_1-2)\left[\int_0^{y_0}[f(y)]^{1/n}\,dy + \int_{y_1}^{y_0}[-f(y)]^{1/n}\,dy\right] +\right.$$
$$+ \int_{y_1}^y\left[\int_1^y\left[\int_{y_1}^y [f(y)]^{1/n}\,dy\right]dy\right]dy + \int_{y_0}^{y_1}\left[\int_{y_0}^y\left[\int_y^{y_0}[-f(y)]^{1/n}\,dy\right]dy\right]dy +$$
$$\left. + \frac{1}{2}(y_1-y_0)^2\int_0^{y_0}[f(y)]^{1/n}\,dy + (y_1-y_0)\int_0^{y_0}\left[\int_0^y [f(y)]^{1/n}\,dy\right]dy + \int_0^{y_0}\left[\int_0^y\left[\int_0^y [f(y)]^{1/n}\,dy\right]dy\right]dy\right] + \theta_T(0)\,. \tag{25}$$

The expression of $\theta_s(y)$, given by

$$\theta_S(y) = Le\frac{C_S}{C_T}\theta_T(y) \tag{26}$$

is obtained by eliminating u from Eq. (17) and (18), and integrating twice the resulting equation taking into account of Eq. (19) and the centro-symmetry of thermal and solutal fields in the core region. The exploitation of such a property and the use of Eq. (26) give, respectively:

$$\theta_T(0) = -C_T E^{1/n}\ Ra_T^{1/n}\left[\frac{(1/2-y_0)^2}{2}\int_0^{y_0}[f(y)]^{1/n}\,dy + \int_{y_0}^{1/2}\left[\int_{y_0}^{y}\left[\int_{y}^{y_0}[-f(y)]^{1/n}\,dy\right]dy\right]dy + \right.$$

$$\left. + (1/2-y_0)\int_0^{y_0}\left[\int_0^{y}[f(y)]^{1/n}\,dy\right]dy + \int_0^{y_0}\left[\int_0^{y}\left[\int_0^{y}[f(y)]^{1/n}\,dy\right]dy\right]dy\right] \quad (27)$$

and

$$\theta_S(0) = Le\frac{C_S}{C_T}\theta_T(0)\,. \quad (28)$$

The expression of $\psi(y)$ can be deduced from that of $u(y)$ by integration of Eq. (6) taking into account of Eq. (10). Therefore, the stream function at the center of the enclosure, which is a measure of the flow intensity, can be expressed by

$$\psi_c = \psi(A/2,1/2) = E^{1/n}Ra_T^{1/n}\left[(1/2-y_0)\int_0^{y_0}[f(y)]^{1/n}\,dy + \int_0^{y_0}\left[\int_0^{y}[f(y)]^{1/n}\,dy\right]dy + \int_{y_0}^{1/2}\left[\int_{y}^{y_0}[-f(y)]^{1/n}\,dy\right]dy\right]. \quad (29)$$

On the other hand, C_T and C_S are evaluated from thermal and solutal boundary conditions imposed on the end walls. Because of the turning flow at the end regions of the fluid layer, the boundary conditions in the *x*-direction, Eq. (9), could not be satisfied by the parallel flow approximation. Instead, the expressions of C_T and C_S are determined by matching the core solution, Eq. (15), to the integral solution for the end regions, which consists on the integration of Eq. (3) and (4), together with the boundary conditions (9) and (10), by considering the arbitrary control volume of Fig. 1. This yields:

$$C_T + 1 = \int_0^1 u(y)\theta_T(y)\,dy$$

and

$$C_S + 1 = Le\int_0^1 u(y)\theta_S(y)\,dy \quad (30)$$

to which the substitution of the expressions of $u(y)$, $\theta_T(y)$ and $\theta_S(y)$ gives:

$$C_T = \frac{1}{A_n E^{1/n} Ra_T^{1/n} - 1} \text{ and } C_S = \frac{1}{A_n Le^2 E^{1/n} Ra_T^{1/n} - 1} \quad (31)$$

On the other hand, knowing that $E = C_T + NC_S$, the following transcendental equation is obtained

$$Le^2 A_n^2 Ra_T^{4/n} E^{1+4/n} - A_n(1+Le^2)Ra_T^{2/n}E^{1+2/n} -$$

$$-(Le^2+N)A_n Ra_T^{2/n}E^{2/n} + E + (N+1) = 0\,, \quad (32)$$

where the coefficient A_n, which depends only on *n*, is calculated with the Gauss-Legendre integration method and its values are presented with those of y_0 in Table 1.

Table 1

Dependence of y_0 and A_n on *n*

n	y_0	A_n
0.6	0.199	$-0.485\cdot10^{-7}$
1.0	0.211	$-0.276\cdot10^{-5}$
1.4	0.219	$-0.160\cdot10^{-4}$

It should be point out, from Table 1, that y_0 is an increasing function of *n*, which means that the velocity maximum is displaced away from the lower wall by increasing *n*. Moreover, Eq. (19)-(27) indicate that *n* is the only parameter that affects the shape of *u*, ψ, θ_T and θ_S profiles.

To determine the value of *E*, Eq. (32) is solved by the Regula-Falsi iteration method and the values of C_T and C_S are deduced from Eq. (31), for each given value of *Le*, *N*, *n* and Ra_T.

Finally, taking into account of Eq. (13) and (14), the Nusselt and Sherwood numbers are constant and can be expressed as

$$Nu = -1/C_T = \overline{Nu}$$

and

$$Sh = -1/C_S = \overline{Sh}\,. \quad (33)$$

Results and discussion

The fact of imposing uniform heat and mass fluxes, as boundary conditions, leads to flow characteristics independent on the aspect ratio, *A*, when this parameter is large enough. The approximate solution, developed in the preceding section, on the basis of the parallel flow assumption, is thus valid asymptotically in the limit of a shallow cavity $A >> 1$. In this respect, after some

numerical tests (results not presented here), 24 is found as being the smallest value of A leading to results reasonably close to those of the large aspect ratio approximation. In fact, the asymptotic analytical limits are largely reached in such a situation. This value reduces to $A = 8$ in pure thermal convection ($N = 0$) as obtained by Lamsaadi et al. [8], which shows the retarding role of the double diffusion with respect to the asymptotic state. On the other hand, for the non-Newtonian fluids considered here, the Prandtl number, Pr, is large enough such that the convection becomes insensitive to any change of the large values of this parameter [4, 8]. On the basis of this, the simulations are conducted with $Pr - \propto$, i.e. by neglecting the convective terms on the left hand side of Eq. (2), which presents the advantage of making the computations faster than with finite large values of Pr [10]. Therefore, the natural double-diffusive convection flow developed inside the enclosure is governed by the thermal Rayleigh number, Ra_T , the buoyancy ratio, N, the Lewis number, Le, and the power-law index n, which is varied, in this study, from 0.6 to 1.4 to include shear-thinning $(0 < n < 1)$, Newtonian $(n = 1)$ and shear-thickening $(n > 1)$ fluids.

Validation of the approximate parallel flow analytical solution

The inspection of the streamlines (*a*) and isotherms (b), depicted in Fig. 2, allows affirming the existence of an analytical solution, for the present problem, owing to the parallelism and the stratification aspects that flow and temperature fields exhibit, respectively, in the central part of the enclosure, i.e. somewhat far from the side edges. Moreover, Fig. 3, comparing the corresponding horizontal velocity (top) and temperature (bottom) profiles, calculated analytically (continuous lines) and numerically (black dots) at mid-length of the cavity, along the vertical direction, testify to the almost perfect agreement between the two types of solutions.

Another confirmation of this is given by Table 2 where the relative difference between analytical and numerical results does not exceed 0.61 % for $|\psi_c|$ and 0.38 % for $\overline{Nu}$.

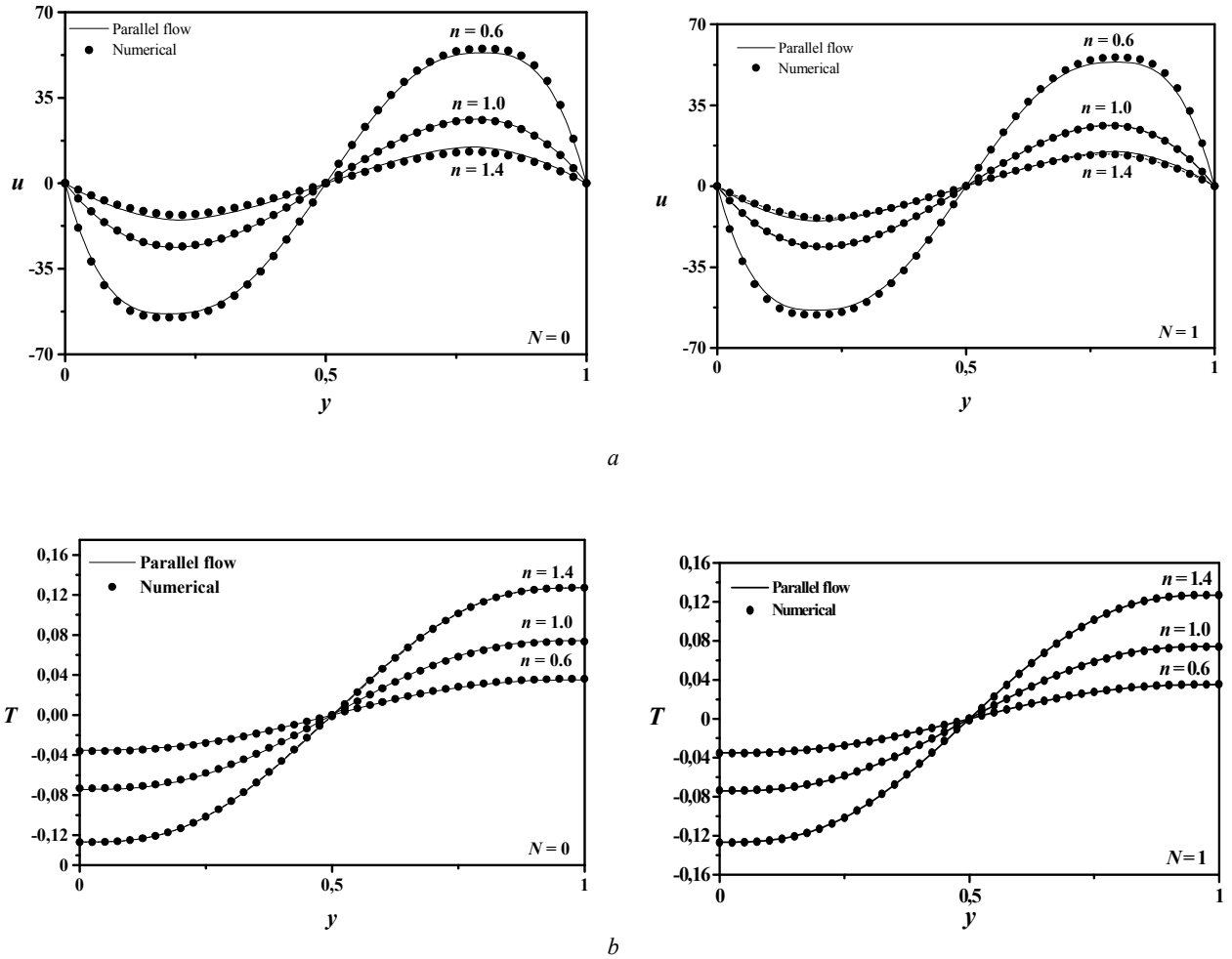

***Fig. 3**. Velocity (a) and temperature (b) profiles for $Ra_T = 10^5$, Le = 10 and different values of n and N*

Table 2

Comparison between the analytical and numerical results for $N = 0$, $Ra_T = 10^5$ and $Le = 10$

$N = 0$		$\lvert\psi_c\rvert$		$\overline{Nu}$	
		Parallel flow	**Numerical**	**Parallel flow**	**Numerical**
n	0.6	19.016	18.991	139,835	139.8
	1.0	8.035	8.01	30.115	30.08
	1.4	4.045	4.02	9.145	9.11
$N = 1$		$\lvert\psi_c\rvert$		$\overline{Nu}$	
		Parallel flow	**Numerical**	**Parallel flow**	**Numerical**
n	0.6	19.1	19.12	140.3	140.33
	1.0	8,51	8.53	30.549	30.58
	1.4	4.57	4.59	9.652	9.68

Hence, it appears clear, from what precedes, that the results of the two approaches adopted in this study agree, at least for the governing parameters selected values, which validates the parallel flow assumption used in section 4 and justifies the choice of $A = 24$ as a large aspect ratio approximation value.

Thermal convection with and without solutal buoyancy forces

At first, it is advisable to recall that the case of natural simple convection (thermal) corresponds to $N = 0$, i.e. the case where solutal buoyancy forces are absent, whereas in presence of these forces, which corresponds to $N \neq 0$, it is about the natural double diffusive convection.

It seems obvious from Fig. 2, where are depicted the streamlines (*a*) and isotherms (*b*), that the flow structure and the thermal field do not undergo qualitative change when N passes from 0 to 1 (case where thermal and solutal buoyancy forces act in the same direction with the same intensity), since the isolines indicate a unicellular regime with a parallel aspect and thermal stratification in the core region of the cavity and this independently on N. The flow and heat transfer intensities, whose numerical values are given in Table 3, show also this fact.

Table 3

Effect of n and N on the flow intensity and heat transfer rate for $Ra_T = 10^5$ and $Le = 10$

		$\lvert\psi_c\rvert$		$\overline{Nu}$	
		$N = 0$	$N = 1$	$N = 0$	$N = 1$
n	0.6	18.991	19.1	139.8	140.3
	1.0	8.01	8.51	30.08	30.549
	1.4	4.02	4.57	9.11	9.652

For a fine examination of the effect of solutal buoyancy forces on thermal convection, the horizontal velocity (*a*) and temperature (*b*)profiles are displayed in Fig. 4.

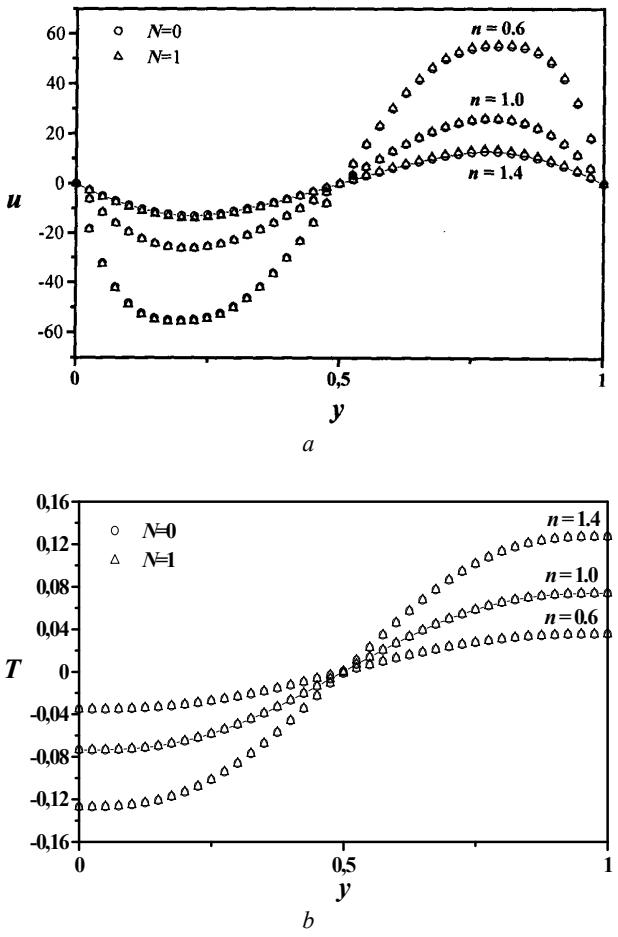

***Fig. 4**. Velocity (a) and temperature (b) profiles for $Ra_T = 10^5$, $Le = 10$ and different values of n and N*

As can be seen, for all the considered values of n, the profiles remain almost identical while passing N from 0 to 1, which means that this parameter does not affect the dynamical and thermal fields. This is related essentially to the fact that the contribution of the solutal effects in the convection is negligible (Le = 10). Such a situation can be described as a regime of prevailing thermal effects.

Influence of the power-law non-Newtonian behaviour on thermal convection

Useful information, concerning the influence of the non-Newtonian rheological behavior on the flow and thermal fields, can be obtained from the examination of Fig. 2. Thus, although the streamlines do not show a qualitative modification in the flow global structure, which keeps a unicellular and parallel aspect in the central part of the cavity independently on the value of n, the flow intensity, ψ_c, undergoes significant quantitative variations with n. In fact $|\psi_c|$ is seen to decrease with n passes, as shown in Table 3, which means, thus, a slowing down of the fluid circulation in such a situation. This trend is confirmed by the velocity profiles (a) of Fig. 3. On the other hand, the corresponding isotherms appear much more affected by the rheological behavior , since they become less and less inclined, with regard to the vertical direction, while increasing n, which testifies, thus, to the reduction of the flow intensity with this parameter. Moreover, Figs. 3 (b) show an increase, in absolute values, of the temperature with n, which indicates that the flow loses its intensity in such circumstances. This type of evolution, with n, is found also on the level of the mean heat transfer rate, $\overline{Nu}$, whose values decrease while increasing n, illustrated by Table 3.

Such results can be explained while referring to Eq. (7), where an increase of n causes an increase of the apparent viscosity, whose slowing-down role on the fluid motion is well known. It results, from what precedes, that, compared to Newtonian case (n = 1), the shear-thinning behavior ($0 < n < 1$) enhances the convection whereas the shear-thickening one ($n > 1$) reduces it.

Conclusion

The present paper is devoted to numerical and analytical experiments on natural simple and double-diffusive convections in a two-dimensional horizontal shallow enclosure ($A >> 1$), filled with non-Newtonian power-law fluids, in the case where both short vertical sides are submitted to uniform heat and mass fluxes while the horizontal boundaries are insulated and impermeable. The main conclusions of the present investigation are summarized as follows:

- The approximate analytical solution, developed on the basis of the parallel flow hypothesis in the core region of the cavity, is found to agree perfectly with the numerical solution, obtained by solving numerically the full governing equations.
- The buoyancy ratio, N, seems not influencing the convection heat transfer while passing from 0 to 1 being given the value of the Lewis number, Le = 10.
- The fluid flow and heat transfer characteristics seem to be rather sensitive to the flow behavior index, n. Thus, compared to Newtonian case (n = 1), the shear-thinning behavior ($0 < n < 1$) enhances the fluid circulation and the convection heat and mass transfers while the shear-thickening one ($n > 1$) produces an opposite effect.

In the future an extent for this study will be carried out with moderate and high values of N in order to examine widely the effect of this parameter on convection heat transfer.

References

1. Viskanta R., Bergman T.L., Incopera F.P. Double-diffusive natural convection. In Natural Convection, Fundamentals and Applications. Hemisphere, Washington DC; 1985.
2. Nield D.A., Bejan A. Convection in Porous Media, Springer Verlag; 1992.
3. Kalla L., Vasseur V., Benacer R., Beji H., Duval R. Double-diffusive convection within a horizontal porous layer salted from the bottom and heated horizontally // Int Comm Heat Mass Transfer. 2001. 28. P. 1-10.
4. Mamou M., Vasseur P., Hasnaoui M. On numerical stability analysis of double-diffusive convection in confined enclosures // J Fluid Mech. 2001. 433. P. 209-250.
5. Ouriemi M., Vasseur P., Bahloul A., Robillard L. Natural convection in a horizontal layer of a binary mixture // Int J Thermal Sciences. 2006. 45. P. 752–759.
6. Benhadji K., Vasseur P. Double-diffusive convection in a shallow porous cavity filled with a non-Newtonian fluid // Int Comm Heat Mass Transfer. 2001. 28. P. 763-772.
7. Ozoe H., Churchill S.W. Hydrodynamic stability and natural convection in Ostwald-De Waele and Ellis fluids: the development of a numerical solution // AIChE J. 1972. 18. P. 1196-1207.
8. Lamsaadi M., Naimi M., Hasnaoui M. Natural convection heat transfer in shallow horizontal rectangular enclosures uniformly heated from the side and filled with non-Newtonian power law fluids // Energy Conversion and Management. 2006. 47. P. 2535-2551.
9. Jaluria Y. Thermal processing of materials: From basic research to engineering // Journal of Heat Transfer. 2003. 125. P. 957-979.
10. Bird R.B., Armstrong R.C., Hassager O. Dynamics of polymeric liquids // Fluid Mechanics. Willey, New York, 1987. Vol. 1.
11. Roache P.J. Computational fluid dynamics. New Mexico, Albuquerque: Hermosa Publishers, 1982.
12. Gourdin A., Boumahrat M. Applied numerical methods. Technique and Documentation-Lavoisier, Paris, 1989.
13. Sibony M., Mardon J-CI. Numerical Analysis II, Approximation and differential equations. Paris: Hermann, 1982.